Applied Physics Letters ARTICLE scitation.org/journal/apl

M-center in low-energy electron irradiated 4*H*-SiC

Cite as: Appl. Phys. Lett. **120**, 252101 (2022); doi: 10.1063/5.0095827
Submitted: 13 April 2022 · Accepted: 13 June 2022 ·
Published Online: 21 June 2022

T. Knežević,[1] A. Hadžipašić,[1,2] T. Ohshima,[3] T. Makino,[3] and I. Capan[1,a)]

AFFILIATIONS

[1]Ruđer Bošković Institute, Bijenička 54, 10 000 Zagreb, Croatia
[2]Faculty of Science, University of Sarajevo, Zmaja od Bosne 33-35, 71 000 Sarajevo, Bosnia and Herzegovina
[3]National Institutes for Quantum Science and Technology, 1233 Watanuki, Takasaki 370-1292, Japan

[a)]Author to whom correspondence should be addressed: capan@irb.hr

ABSTRACT

We report on the low-energy electron irradiated 4*H*-SiC material studied by means of deep-level transient spectroscopy (DLTS) and Laplace-DLTS. Electron irradiation has introduced the following deep level defects: EH_1 and EH_3 previously assigned to carbon interstitial-related defects. We propose that EH_1 and EH_3 are identical to M_1 and M_3, also recently assigned to carbon interstitial defects, and assign them to $C_i^{=}(h)$ and $C_i^{0}(h)$, respectively.

Electrically active defects in n-type 4*H*-SiC have been studied in detail for decades. Piece by piece, the puzzle behind the most common and dominant defect traps, such as $V_C(=/0)$, $V_C(0/++)$, and V_{Si}, has been solved. Part of the puzzle that has kept researchers busy for several years is the study of silicon vacancy and carbon interstitial defects (V_{Si} and C_i), introduced by radiation. It was well known that electron irradiation,[1–3] proton irradiation,[4–6] neutron irradiation,[7,8] and ion implantation[9,10] introduce two deep level defects in the n-type 4*H*-SiC material. These levels are located at 0.40 and 0.70 eV below the conduction band and have been labeled either as $S_{1/2}$ or $EH_{1/3}$. Recently, Bathen *et al.*[6] have provided conclusive evidence that $S_{1/2}$ deep level defects are related to V_{Si}, while Alfieri and Mihaila[3] have shown that $EH_{1/3}$ deep level defects are related to C_i. The $EH_{1/3}$ deep level defects are introduced only in the case of the low-energy electron irradiation (<200 keV), since under such conditions, silicon atoms cannot be displaced.[1,2]

The V_{Si} has attracted much attention in recent years due to its physical properties and its potential application for quantum sensing.[6,11–13] The S_1 and S_2 are identified as V_{Si} $(-3/=)$ and V_{Si} $(=/-)$ charge transitions, respectively. Bathen *et al.*[6] have shown that S_1 (in proton irradiated 4*H*-SiC samples) has two emission lines originating from V_{Si} sitting at $-k$ and $-h$ lattice sites. These findings were later confirmed by Capan *et al.*[8] when studying 4*H*-SiC material irradiated with fast neutrons.

Despite their technological importance, C_i defects are not yet fully understood. Coutinho *et al.*[14] have recently shown that a bistable defect in 4*H*-SiC, known as M-center, is carbon interstitial. Accordingly, the defect is responsible for two pairs of the first and second acceptor transitions[4,5,10,14,15]

Configuration A

$$\rightarrow \{M_1(=/-) = E_c - 0.42\,\text{eV};\ M_3(-/0) = E_c - 0.74\,\text{eV}\},$$

Configuration B

$$\rightarrow \{M_2(=/-) = E_c - 0.65\,\text{eV};\ M_4(-/0) = E_c - 0.86\,\text{eV}\},$$

where configurations A and B were assigned to a carbon interstitial at the hexagonal and cubic sub-lattice sites, $C_i(h)$ and $C_i(k)$, respectively. The two configurations can be interchanged by annealing and applying a reverse bias voltage. Configuration A is obtained when the measurement is performed after annealing the sample just above room temperature under reverse bias voltage. The defect jumps to configuration B after the sample is annealed at ∼450 K without bias.

The evident similarities between $M_{1/3}$ and $EH_{1/3}$ traps, including their location within the bandgap and their formation conditions, are so striking that we must hypothesize that they may ultimately arise from the same defect. Therefore, the main goal of this work is twofold. By using low energy electrons and low fluence, we intend to introduce only the $EH_{1/3}$ deep level defects and verify if there is evidence for bistability and the formation of $M_{1/3}$. Moreover, since we displace only the carbon atoms, resulting in a very clear EH_1 signal, Laplace-deep-level transient spectroscopy (DLTS) was used to investigate possible superposition of EH_1 and M_1 signals.

In this work, n-type Schottky barrier diodes (SBDs) were fabricated on nitrogen-doped ($\sim 4.7 \times 10^{14}\,cm^{-3}$) 4*H*-SiC epitaxial layers, with a thickness of approximately 25 μm. The epi-layer was grown on an 8° off-cut silicon face of a 350 μm thick 4*H*-SiC (0001) wafer without a buffer layer by chemical vapor deposition. The Schottky barriers were formed by thermal evaporation of nickel through a metal mask with a patterned squared aperture of 1 mm edge length, while the Ohmic contacts were formed on the backside of the silicon carbide substrate by nickel sintering at 950 °C in an Ar atmosphere.

Low-energy electron irradiations were performed at Nissin Electric Group (NEG), Kyoto, Japan. The electron energy was 150 keV, and the total fluence was $1 \times 10^{15}\,cm^{-2}$. The irradiations have been performed through the Schottky contact (Ni, thickness $\leq$ 100 nm) at room temperature (RT).

DLTS measurements were performed using a Boonton 7200 capacitance meter (Boonton Electronics, New Jersey, USA) and an National Instruments PCI-6521 data acquisition device (NI, Austin, USA). Conventional DLTS measurements were carried out in the temperature range of 100 to 450 K with a temperature ramp rate of 2 K/min. Reverse voltage, pulse voltage, and pulse width were $V_R = -4$V, $V_P = 0$ V, and $t_P = 10$ ms, respectively. For the Laplace-DLTS measurements, the following acquisition settings were used: the number of samples 3×10^4, the sampling rate 10–80 kHz, and the number of averaged scans 100–800. The numerical routine FLOG[16] was used to calculate Laplace-DLTS spectra.

M-center was transformed to configuration B and configuration A by annealing at 450 K (for 20 min) and cooling the SBD without applying a bias voltage (0 V), or by annealing at 340 K for 20 min and cooling down the SBD with an applied bias voltage of −30 V, respectively.

Figure 1 shows the DLTS spectrum for the as-grown n-type 4*H*-SiC SBD. In the as-grown sample, only the $Z_{1/2}$ peak is present. The $Z_{1/2}$ has already been reported in numerous studies and assigned to $V_c(=/0)$.[17–19]

Figure 2 shows the DLTS spectrum for the n-type 4*H*-SiC SBD irradiated with low-energy electrons in configurations A and B. The DLTS measurement of the as-irradiated sample (without pre-measurements bias and annealing settings needed for the configuration A and configuration B) is not shown here. The measurements did not reveal any new information, and they are similar to the spectra shown in Fig. 2.

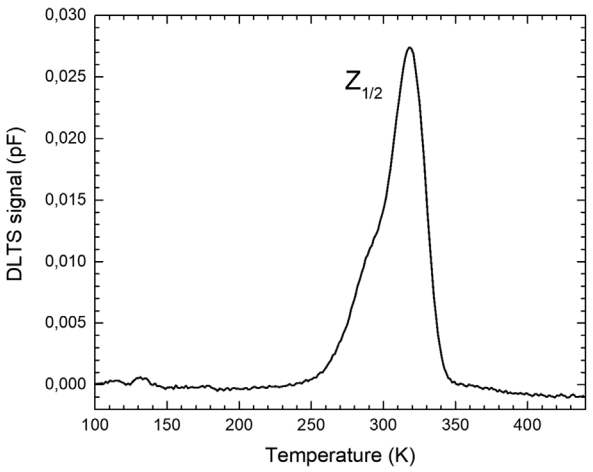

FIG. 1. DLTS spectrum for the as-grown 4*H*-SiC sample. Reprinted from Capan *et al.*, J. Appl. Phys. **124**, 245701 (2018). Copyright 2018 AIP Publishing.

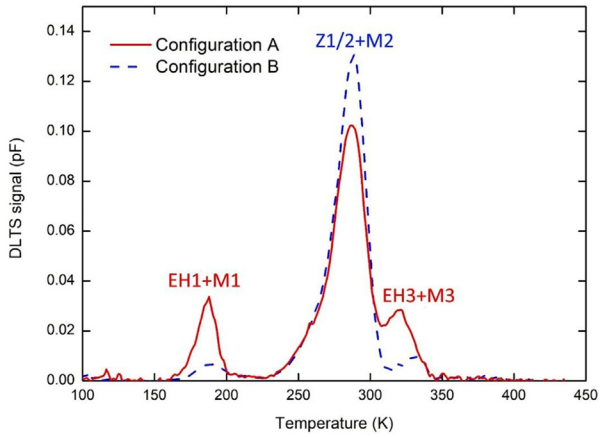

FIG. 2. DLTS spectra for the 4*H*-SiC sample irradiated with low-energy electrons, measured in configurations A and B.

The low-energy electron irradiation has increased the concentration of $Z_{1/2}$. The obtained concentration of $\sim 10^{12}\,cm^{-3}$ is in a good agreement with previously reported studies.[3] Moreover, irradiation introduced two deep-level defects, whose positions (0.41 and 0.70 eV) are close to those that are usually labeled as EH_1 and EH_3. However, the observed peaks are also metastable and consistent with the properties of the M-center.[4,5,10,14,15] The spectra depend on the applied bias voltage and annealing. The bistable defect, known as M-center, introduces four electrically active deep-level defects. M_1 and M_3 overlap with EH_1 and EH_3 in configuration A, while M_2 overlaps with $Z_{1/2}$ in configuration B (Fig. 2). M-states and their bi-stability are more clearly observed if the DLTS signal difference (configuration A − configuration B) is plotted, as shown in Fig. 3. As previously reported, it is not possible to observe the M_4 with DLTS due to the technical limitations, but M_4 has been observed in ion-implanted[10] and neutron-irradiated[8] 4*H*-SiC using the isothermal DLTS.

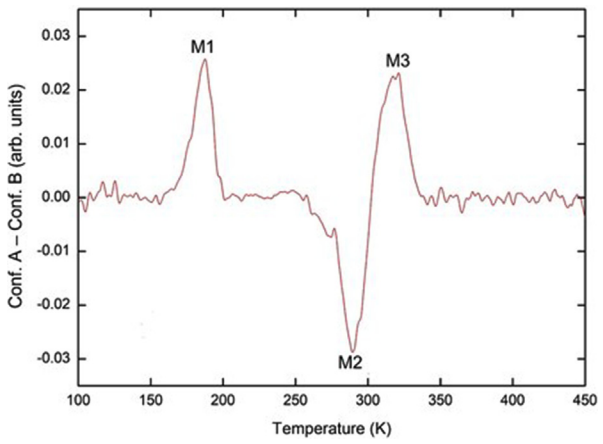

FIG. 3. The DLTS signal difference (configuration A—configuration B) for the 4*H*-SiC sample irradiated with low-energy electrons.

We have estimated the activation energies for M_1, M_2, and M_3 and obtained the following values 0.42, 0.73, and 0.90 eV, which are consistent with previously reported values.[4,5,10,14,15]

The DLTS data obtained in this study are in perfect agreement with previous results from DLTS studies on low-energy electron irradiated 4H-SiC samples.[1] However, triggered by the recent advancements in understanding and identifying the M-center,[14] accompanied by the recent progress in understanding the $EH_{1/3}$ and $S_{1/2}$ defects,[3,6] we have applied the Laplace-DLTS technique to study the EH_1 in more details and to investigate the correlation between the EH_1 and the M_1 defect.

Figure 4 shows Laplace-DLTS spectra in configurations A and B, measured at the temperature of the EH_1 DLTS peak (T = 200 K). The Laplace-DLTS results clearly indicate that EH_1 defect has a single emission line, with no splitting of the emission line due to the different lattice sites ($-h$ and $-k$) as is the case for S_1 and/or $Z_{1/2}$ ($EH_{6/7}$).[6,8,17,18,20] Thus, our results clearly show that Laplace DLTS can be used as a tool to distinguish S_1 (not shown here) and EH_1, which give identical signals in the DLTS spectrum. This is the first time that EH_1 has been directly measured with Laplace-DLTS.

According to the recent findings of Coutinho *et al.*,[14] the M-center was assigned to C_i. The four states arising from the M-center are assigned to different charge states located at the different lattice sites. M_1 and M_3 are assigned to $C_i^{=}(h)$ and $C_i^{0}(h)$, while M_2 and M_4 are assigned to $C_i^{=}(k)$ and $C_i^{0}(k)$. The occupancy of the $-h$ or $-k$ lattice sites is controlled by the reverse bias voltage anneals. For example, if we perform zero bias annealing (configuration B), the $-k$ sites will be dominantly occupied, leading to the appearance of M_2 and M_4 in the DLTS spectra. However, if we perform reverse bias annealing (configuration A), then the occupation of the $-h$ sites prevails, which gives rise to M_1 and M_3 in the DLTS spectra.

According to the Laplace-DLTS measurements at temperatures around 200 K (i.e., temperature at which EH_1 has the peak maximum in the DLTS spectrum), only one emission line is observed in both configurations, A and B. There is no convincing evidence or even suggestions for two overlapping defects with identical emission lines that

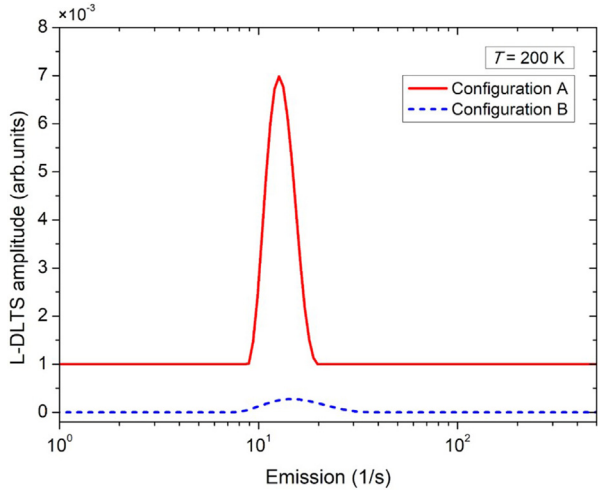

FIG. 4. Laplace DLTS spectra of the 4*H*-SiC samples irradiated with low-energy electrons, measured in configurations A and B at a measurement temperature of 200 K.

are unresolved by Laplace-DLTS. Let us assume that M_1 is indeed EH_1. The difference in the intensity of EH_1 peak (DLTS spectra) in configurations A and B is not due to the overlap of an additional defect, such as M_1, but to the different occupancy of $C_i^{=}(h)$ sites. For configuration A, as explained above, this is more favorable than $-k$ sites. Therefore, we can speculate that EH_1 is the same defect as M_1 and assigned to $C_i^{=}(h)$.

Based on the difference signal (configuration A—configuration B), as shown in Fig. 3, the concentrations of M_1 and M_2 are identical within the measurements error margin. M_2 has been recently assigned to $C_i^{=}(k)$.[7] This leads us to conclusion that conversion $C_i^{=}(h) \leftrightarrow C_i^{=}(k)$ occurs more easily than anticipated. As mentioned above, we control the occupancy of the $-h$ and $-k$ sites by different bias voltage annealing. From isothermal annealing, the conversion from configuration A to configuration B was previously measured to be activated with a barrier of 1.4 eV, while the conversion from configuration B to configuration A is activated with a lower barrier of 0.9 eV[4]. It should be noted that these values were estimated in the study of the MeV proton implanted 4*H*-SiC material. The MeV implantations result in the introduction of the $S_{1/2}$ defects (V_{Si}). By varying the filling pulse length while maintaining the measurement temperature at the S_1/M_1 peak position, Martin *et al.*[4] have clearly shown that contributions from at least two different defects, S_1, and M_1 are present in configuration B. These results were recently confirmed by Capan *et al.*[8] as S_1 and M_1 have directly been measured with Laplace-DLTS. Not only do we have contributions from S_1 and M_1, but S_1 is additionally resolved into two components. Although the analysis of the conversion barriers (configuration A ↔ configuration B) has been done using the "difference" DLTS signal (presumably this is the case where the signal is only due to the M-center),[4] we should not completely underestimate the fact that the conversion barriers were not determined under conditions equivalent to those reported in this study. The conversion barriers $C_i^{=}(h) \leftrightarrow C_i^{=}(k)$ could be lower than previously assumed.

All these results imply that $EH_{1/3}$ and M-center are indeed carbon interstitials, and they are all arising from the same defects. Thus, we conclude that EH_1 and EH_3 are identical to M1 and M3 and assign them to $C_i^{=}(h)$ and $C_i^{0}(h)$, respectively.

Unfortunately, Laplace-DLTS cannot provide conclusive information about EH_3 as is the case with EH_1, since the EH_3 is too close to $Z_1(=/0)$ and $Z_2(=/0)$ in the Laplace DLTS spectrum, and they overlap. The conversion $C_i^{0}(h) \leftrightarrow C_i^{0}(k)$ should follow the same path. Further studies with isothermal DLTS are needed since this is the only way to measure M_4 directly.

In this work, we have used DLTS and Laplace-DLTS to study carbon interstitial-related defects ($EH_{1/3}$ and $M_{1/3}$) in the low-energy electron irradiated 4*H*-SiC material. Based on the results obtained in this study, we propose that EH_1 and EH_3 are identical to M_1 and M_3 and assign them to $C_i^{=}(h)$ and $C_i^{0}(h)$, respectively.

This work was supported by the North Atlantic Treaty Organization Science for Peace and Security Program through Project No. G5674.

AUTHOR DECLARATIONS

Conflict of Interest

The authors have no conflicts to disclose.

Author Contributions

T. Knežević: Formal analysis (equal); Investigation (equal). **A. Hadžipašić:** Data curation (equal); Formal analysis (equal). **T. Ohshima:** Investigation (equal); Methodology (equal); Resources (equal). **T. Makino:** Data curation (equal); Investigation (equal). **I. Capan:** Conceptualization (equal); Supervision (equal); Writing – original draft (equal); Writing – review and editing (equal).

DATA AVAILABILITY

The data that support the findings of this study are available from the corresponding author upon reasonable request.

REFERENCES

[1]F. C. Beyer, C. Hemmingsson, H. Pedersen, A. Henry, E. Janzén, J. Isoya, N. Morishita, and T. Ohshima, J. Appl. Phys. **109**, 103703 (2011).
[2]G. Alfieri, E. V. Monakhov, B. G. Svensson, and M. K. Linnarsson, J. Appl. Phys. **98**, 043518 (2005).
[3]G. Alfieri and A. Mihaila, J. Phys. Condens. Matter **32**, 465703 (2020).
[4]M. L. David, G. Alfieri, E. M. Monakhov, A. Hallén, C. Blanchard, B. G. Svensson, and J. F. Barbot, J. Appl. Phys. **95**, 4728 (2004).
[5]D. M. Martin, H. Kortegaard Nielsen, P. Lévêque, A. Hallén, G. Alfieri, and B. G. Svensson, Appl. Phys. Lett. **84**, 1704 (2004).
[6]M. E. Bathen, A. Galeckas, J. Müting, H. M. Ayedh, U. Grossner, J. Coutinho, Y. K. Frodason, and L. Vines, npj Quantum Inf. **5**, 111 (2019).
[7]I. Capan, T. Brodar, Y. Yamazaki, Y. Oki, T. Ohshima, Y. Chiba, Y. Hijikata, L. Snoj, and V. Radulović, Nucl. Instrum. Methods Phys. Res. Sect. B Beam Interact. Mater. Atoms. **478**, 224 (2020).
[8]I. Capan, T. Brodar, T. Makino, V. Radulovic, and L. Snoj, Crystals **11**, 1404 (2021).
[9]Z. Pastuović, R. Siegele, I. Capan, T. Brodar, S. Sato, and T. Ohshima, J. Phys.: Condens. Matter **29**, 475701 (2017).
[10]I. Capan, T. Brodar, R. Bernat, Ž. Pastuović, T. Makino, T. Ohshima, J. D. Gouveia, and J. Coutinho, J. Appl. Phys. **130**, 125703 (2021).
[11]J. Wang, Y. Zhou, X. Zhang, F. Liu, Y. Li, K. Li, Z. Liu, G. Wang, and W. Gao, Phys. Rev. Appl. **7**, 064021 (2017).
[12]M. Widmann, S. Y. Lee, T. Rendler, N. T. Son, H. Fedder, S. Paik, L. P. Yang, N. Zhao, S. Yang, I. Booker *et al.*, Nat. Mater. **14**, 164 (2015).
[13]F. Fuchs, B. Stender, M. Trupke, D. Simin, J. Pflaum, V. Dyakonov, and G. V. Astakhov, Nat. Commun. **6**, 7578 (2015).
[14]J. Coutinho, J. D. Gouveia, T. Makino, T. Ohshima, Ž. Pastuović, L. Bakrač, T. Brodar, and I. Capan, Phys. Rev. B **103**, L180102 (2021).
[15]H. K. Nielsen, A. Hallén, and B. G. Svensson, Phys. Rev. B **72**, 085208 (2005).
[16]L. Dobaczewski, A. R. Peaker, and K. B. Nielsen, J. Appl. Phys. **96**, 4689 (2004).
[17]I. Capan, T. Brodar, Z. Pastuović, R. Siegele, T. Ohshima, S. I. Sato, T. Makino, L. Snoj, V. Radulović, J. Coutinho, V. J. B. Torres, and K. Demmouche, J. Appl. Phys. **123**, 161597 (2018).
[18]I. Capan, T. Brodar, J. Coutinho, T. Ohshima, V. P. Markevich, and A. R. Peaker, J. Appl. Phys. **124**, 245701 (2018).
[19]N. T. Son, X. T. Trinh, L. S. Løvlie, B. G. Svensson, K. Kawahara, J. Suda, T. Kimoto, T. Umeda, J. Isoya, T. Makino, T. Ohshima, and E. Janzén, Phys. Rev. Lett. **109**, 187603 (2012).
[20]G. Alfieri and T. Kimoto, Appl. Phys. Lett. **102**, 152108 (2013).